Journal of Sound and Vibration (1997) **202**(5), 605–618

WALL-BOUNDED BLADE-TIP VORTEX INTERACTION NOISE

R. C. Dunne and M. S. Howe

Boston University, *College of Engineering*, 110 *Cummington Street*, *Boston*, *MA* 02215, *U.S.A.*

(*Received* 28 *August* 1995, *and in final form* 15 *August* 1996)

An analytical treatment is given of the canonical problem of the generation of sound when a locally rectilinear vortex is drawn through the clearance gap between a wall and the square tip of a rigid blade at low Mach number. The mean flow in the neighborhood of the blade tip is assumed to be locally two-dimensional, and is modelled by free streamline potential flow theory, according to which the flow into the gap on the pressure side emerges as a wall jet on the suction side. The additional vorticity shed from the tip (in accordance with the unsteady Kutta condition) during the passage of the vortex is assumed to convect at constant speed along the free streamline boundary of the jet. Sound is generated by a dipole source, the magnitude and orientation of which are determined by the unsteady lift experienced by the blade. We calculate the separate contributions to the radiation (i.e., to the dipole strength) from the vortex and the shed vorticity. The sound is generated while the vortex is within a distance from the blade tip comparable to the clearance, and has wavelength which is order $1/M$ larger, where M is the characteristic Mach number of the flow. The conclusions of this analysis are supported by an alternative, simplified treatment in which the vortex motion through the gap is assumed to be steady and the shed vorticity convects at a fixed distance from the duct wall rather than along the free streamline.

1. INTRODUCTION

An important mechanism of sound production by rotors and fixed control surfaces is related to unsteady surface forces induced by turbulence and discrete vortices [1–3]. To estimate the level and character of the sound the flow must normally be determined by numerical integration of the coupled Navier–Stokes equations and the stuctural equations of motion. However, a small number of canonical fluid–structure interaction problems can be treated analytically, typically when the Mach number is small, and their solutions are of considerable value in assessing the efficiency and accuracy of different numerical schemes.

When the working fluid is uniform, the principal aerodynamic sound sources in turbomachines are quadrupole volume sources, the strengths of which are proportional to the turbulence Reynolds stress, and dipoles distributed over solid surfaces. At low Mach numbers the dipoles are usually dominant, and various analytical techniques have been developed to estimate their contributions (e.g., see references [4–14]). In modelling such interactions it is known that the motions and strengths of all of the vorticity interacting with a surface must be included; in particular, it is usually necessary to take proper account of additional vorticity generated at the surface during the interaction. For example, vortex shedding from the trailing edge is known to have a considerable influence on the unsteady lift experienced by an airfoil passing through a turbulent gust, and therefore on the sound produced during blade–vortex interactions [15].

0022–460X/97/200605 + 14 $25.00/0/sv960791

In this paper we investigate analytically the canonical problem of the sound generated when a vortex, shed, perhaps, from an appendage in a low Mach number duct flow (see Figure 1), is entrained by the mean flow between a blade tip and wall. This regime is just one of several possible rotor blade–vortex interactions that generate sound (the most common involving the ingestion and possible "chopping" of the vortex by blades), and is particularly important in underwater applications. The clearance between the blade and wall is taken to be uniform, and the vortex is assumed to be forced at high Reynolds number through the rectangular shaped gap between the blade tip and wall. Relative to the blade, the vortex is accelerated into the gap on the pressure side of the blade within a locally two-dimensional "sink" flow, and emerges at high speed on the suction side within a wall-jet. During this unsteady interaction additional vorticity is shed into the jet from the blade tip. Both the "incident" and shed vorticity produce unsteady forces on the blade, and the aggregate force determines the strength of the equivalent acoustic dipole source. To calculate the value of this force it is assumed that the shed vorticity convects within a thin vortex sheet in the shear layer of the wall jet, and the vortex sheet strength is obtained by application of the Kutta condition at the blade tip. The analytical problem is similar to one investigated by Obermeier and von Schroeter [5], who examined the sound produced during vortex motion through an infinitely long slit in a rigid plane, although no account was taken of mean flow, nor of vortex shedding from the edges of the aperture.

The blade–vortex interaction is discussed in section 2, where the motion of the vortex through the gap is determined by numerical integration of its equations of motion, and the strength of the shed vorticity is calculated. The sound generated by the interaction is estimated in section 3, and a comparison is made (in section 4) with the results of a simpler approximation in which the vortex is assumed to translate at constant velocity relative to the blade. Estimates given in section 4 indicate that the amplitude of the radiation is comparable to that produced when the same vortex is chopped by the blade. Appendix A contains a brief derivation of the acoustic Green's function used in the calculations.

2. THE BLADE–VORTEX INTERACTION

2.1. FORMULATION OF THE PROBLEM

A rotor with nominally rigid blades is located with its axis of rotation on the centerline of a circular cylindrical duct in the presence of a low Mach number mean axial flow. An axially orientated vortex is assumed to pass through the rotor plane between the duct wall and the blade tips. It is required to estimate the aerodynamic sound generated when a blade tip passes over the vortex.

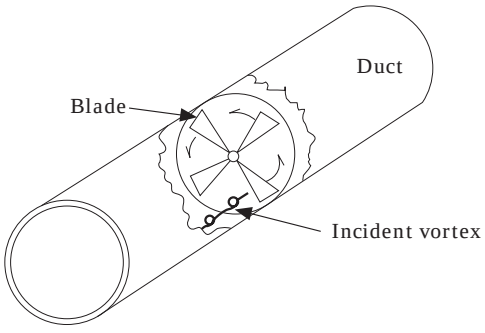

Figure 1. A schematic of blade–vortex interaction in a duct.

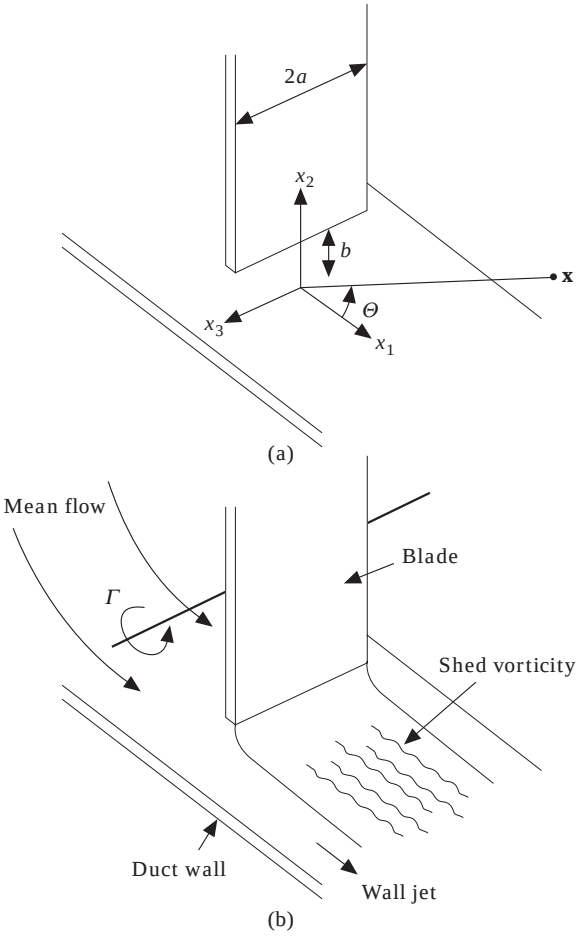

Figure 2. (a) The local co-ordinate system used to specify the interaction of the vortex and blade. (b) A schematic of the local two-dimensional model.

The problem is simplified by means of the following hypotheses: (1) the duct is rigid and sufficiently large that the influence of wall curvature may be neglected in the interaction region; (2) a blade may be modelled as a rectangular strip of chord $2a$, with a uniform clearance $b \ll a$ between the tip and duct wall; (3) the impinging vortex is aligned with the blade chord during the interaction; (4) the vortex core radius is negligible.

To analyze the interaction with a single blade, introduce the local rectangular co-ordinate system (x_1, x_2, x_3) illustrated in Figure 2(a), the co-ordinate origin being at the wall, symmetrically placed with respect to the blade. The x_1-axis is normal to the blade, and the x_2-axis is directed radially inwards towards the rotor axis. The blade motion causes fluid to be forced through the gap between the blade tip and the wall in the positive x_1-direction, as indicated in Figure 2(b). Since $b \ll a$, the relative fluid motion near the blade tip resembles a two-dimensional sink-flow into the gap from $x_1 < 0$ and a wall jet in $x_1 > 0$. This high Reynolds number mean flow will be modelled locally by the two-dimensional, incompressible, free streamline potential flow through a slit of width $2b$ in an infinite plane [16, 17].

2.2. MOTION OF THE VORTEX

Let the incident vortex have circulation Γ. The vortex motion through the gap according to potential theory is calculated by the method of conformal transformation. This motion is composed of three components: the induced velocity due to image vortices in the duct wall and blade; convection by the mean free-streamline flow through the gap; and induced motion caused by vorticity shed from the blade tip in accordance with the Kutta condition. The last of these will be ignored, since it can be significant only after passage of the vortex through the gap, when, however, the motion becomes dominated by the high speed jet.

Let $z_0(t) = x_0(t) + \mathrm{i}y_0(t)$ denote the position of the vortex at time t in the complex plane $z = x_1 + \mathrm{i}x_2$. By the usual procedure [16, 17] (details are given in reference [18]), when the influence of unsteady vortex shedding is ignored, the equation of motion of the vortex can be cast in the form

$$\frac{\mathrm{d}x_0}{\mathrm{d}t} - \mathrm{i}\frac{\mathrm{d}y_0}{\mathrm{d}t} = \frac{3\mathrm{i}\Gamma z_0}{4\pi(z_0^2 + b^2)} + \frac{\mathrm{i}\Gamma}{2\pi(z_0^2 + b^2)^{3/2}} \Bigg/ \left(\frac{z_0}{\sqrt{(z_0^2 + b^2)}} - \text{c.c.} \right) + U_{jet} - \mathrm{i}V_{jet}, \qquad (1)$$

where "c.c." denotes the complex conjugate of the preceding quantity. The first two terms on the right side represent the volocity induced by images in the rigid surfaces; $U_{jet} - \mathrm{i}V_{jet} = \mathrm{d}w/\mathrm{d}z$ (evaluated at $z = z_0$), where $w(z)$ is the velocity potential of the free streamline flow through the gap, which is determined by the solution of

$$\frac{\mathrm{d}w}{\mathrm{d}z} = \mathrm{i}V/\sigma(\mathrm{i}\exp(-\pi w/2bV) + [\{\mathrm{i}\exp(-\pi w/2bV)\}^2 - 1]^{1/2}), \qquad (2)$$

where V is the mean velocity (relative to the blade) in the jet in the plane of the gap, and $\sigma = \pi/(\pi + 2) \approx 0{\cdot}61$ [16, 17] is the contraction ratio, defined such that the asymptotic jet velocity is V/σ. Equation (2) can be integrated numerically to determine $w = w(z)$ from the initial condition $w = \mathrm{i}bV$ at $z = \mathrm{i}b$ (at the blade tip), and the solution used in equation (1) to find the path of the vortex.

The results of such calculations are illustrated in Figure 3. Three typical vortex trajectories $(X(t),\ Y(t)) = (x_0(t),\ y_0(t))/b$ are shown for the case $\Gamma = (5\pi/9)Vb \approx 1{\cdot}75Vb$. The vortex is released at a large, non-dimensional negative time Vt/b and allowed to

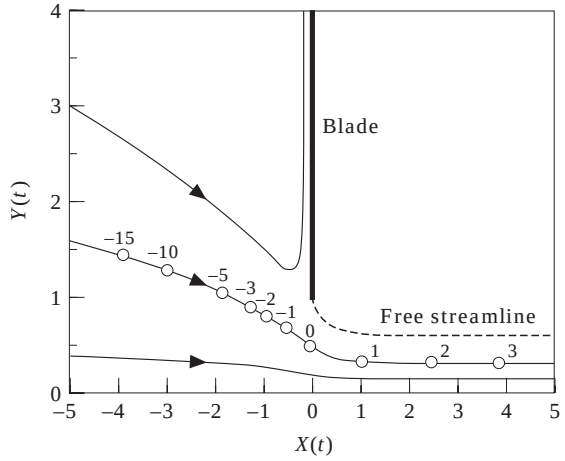

Figure 3. Typical vortex trajectories for various initial positions of the vortex as $X = x/b \to -\infty$. The open circles denote vortex positions at different non-dimensional times Vt/b for $\Gamma = 1{\cdot}75Vb$, $d/b = 0{\cdot}5$.

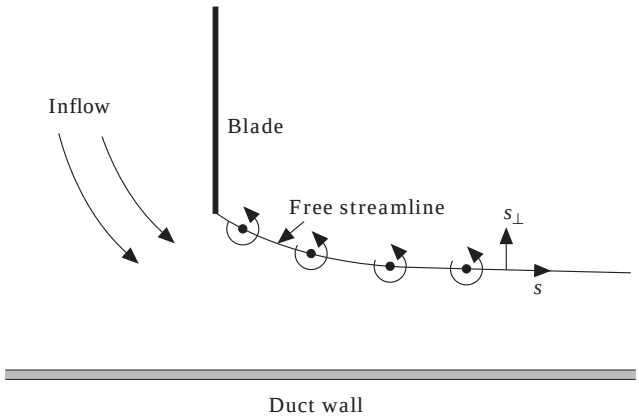

Figure 4. A schematic illustration of shed vortex elements convecting along the free streamline of the wall jet.

translate towards the gap from $x_1 < 0$. If the starting position is too far from the duct wall, the vortex does not penetrate the gap (as exemplified by the upper trajectory in the figure). When the starting position is close to the wall, the trajectory is uniform until the vortex enters the gap, where the concentration of the jet brings it closer to the wall. The open circles on the intermediate trajectory shown in the figure denote positions of the vortex at different times Vt/b ($t = 0$ as the vortex crosses the plane of the gap at a distance $d = 0{\cdot}5b$ from the duct wall), and illustrate the acceleration of the vortex as it approaches and enters the gap.

2.3. THE SHED VORTICITY

Unsteady vorticity shed from the blade tip during the passage of the vortex through the gap is assumed to form a vortex sheet along the undisturbed free streamline of the wall jet, as indicated schematically in Figure 4. The mean flow speed just inside the jet at this streamline is constant and equal to V/σ; we shall assume that the shed vorticity convects along the free streamline at speed $V_c = V/2\sigma$, which is marginally smaller than the mean velocity in the plane of the gap. If s denotes the distance measured along the free streamline from the blade tip, the shed vorticity can be represented in the form

$$\mathbf{\Omega} = \gamma(t - s/V_c)\delta(s_\perp)\mathbf{k}, \tag{3}$$

where $\gamma(t - s/V_c)$ is the unsteady component of the circulation per unit distance along the free streamline, $s_\perp$ denotes distance measured in the normal direction from the streamline, and $\mathbf{k}$ is a unit vector in the x_3-direction.

The Kutta condition is applied at the blade tip by equating to zero the sum of the singular velocities induced at the tip by the vortex Γ and the shed vorticity. The procedure is similar in principle to the application of the Kutta condition at the trailing edge of a thin airfoil subject to gust loading [19], and leads to the following integral equation for γ:

$$\Gamma(\mathrm{i}\zeta_0 + \text{c.c.}) + \int_0^\infty \gamma(t - s/V_c)(\mathrm{i}\zeta_s + \text{c.c.})\,\mathrm{d}s = 0, \tag{4}$$

where ζ_0 and ζ_s, respectively, denote the function

$$\zeta = z/(z^2 + b^2)^{1/2} \tag{5}$$

evaluated at the current complex position $z_0(t)$ of the vortex, and at the point z_s on the free streamline which is at distance *s along the streamline* from the blade tip.

Equation (4) is solved by writing

$$\gamma(t - s/V_c) = \int_{-\infty}^{\infty} \gamma_0(\omega)\, \mathrm{e}^{-\mathrm{i}\omega(t - s/V_c)}\, \mathrm{d}\omega, \tag{6}$$

and taking the Fourier transform of equation (4) with respect to time. This yields

$$\gamma_0(\omega) = \frac{-\Gamma \displaystyle\int_{-\infty}^{\infty} [\mathrm{i}\zeta_0(t) + \text{c.c.}]\, \mathrm{e}^{\mathrm{i}\omega t}\, \mathrm{d}t}{2\pi \left\{ \displaystyle\int_0^{\infty} [\mathrm{i}\zeta_s + \text{c.c.}] \exp(\mathrm{i}\omega s/V_c)\, \mathrm{d}s \right\}}. \tag{7}$$

Both of the integrals on the right side must be evaluated numerically, making use of the numerical solution of equation (1) for the position $z_0(t)$ of the vortex Γ at time t, and of the parametrization of the point z_s on the free streamline in terms of the distance s (see reference [18] for details).

3. THE AERODYNAMIC SOUND

3.1. THE ACOUSTIC ANALOGY

When the vorticity $\mathbf{\Omega}$ is known as a function of position and time, the aerodynamically generated sound in low Mach number flow is conveniently calculated from the acoustic analogy equation in the form [14]

$$\{\partial^2/c_0^2\, \partial t^2 - \nabla^2\} B = \mathrm{div}(\mathbf{\Omega} \wedge \mathbf{v}), \tag{8}$$

where c_0 is the speed of sound, $\mathbf{v}$ is the velocity, $B = w + \frac{1}{2}v^2$ is the total enthalpy, and w is the specific enthalpy. When the specific entropy is uniform (as assumed in the present problem), the local fluid density ρ is a function of the pressure p alone, and $w = \int \mathrm{d}p/\rho(p)$. Bernoulli's equation [16, 17] then shows that $B \equiv -\partial\varphi/\partial t$ in those regions where the flow is irrotational and defined by a velocity potential φ. B is therefore *constant* in steady irrotational flow, and far from the interaction region perturbations in B represent radiating sound waves. When the mean flow Mach number is negligible the acoustic pressure at large distances from the source flow $p \approx \rho_0 B$, where ρ_0 is the mean density.

In the same low Mach number approximation, the motion of the blade may be ignored in calculating the radiated sound, since it is then only the relative motions of the blade and vortices that determine the radiated sound [13]. This is because at very low Mach numbers the motion close to the blade is essentially incompressible (as assumed in equation 2), and the unsteady surface forces (i.e., the aeroacoustic dipole source strengths) are determined by the relative motion of the blade and fluid. Thus, in calculating the radiation we may assume the blade to be at rest, in which case it is clear from the identification $B \equiv -\partial\varphi/\partial t$ ($\mathbf{\Omega} = \mathbf{0}$) that B must have vanishing normal derivatives on the blade and duct wall.

The solution of equation (8) which satisfies this condition together with the radiation condition of outgoing wave behavior can be cast in the form

$$B(\mathbf{x}, t) = -\int\int (\mathbf{\Omega} \wedge \mathbf{v})(\mathbf{y}, \tau) \cdot \frac{\partial G}{\partial \mathbf{y}}(\mathbf{x}, \mathbf{y}, t - \tau)\, \mathrm{d}^3\mathbf{y}\, \mathrm{d}\tau, \tag{9}$$

where the Green function $G(\mathbf{x}, \mathbf{y}, t, -\tau)$ has vanishing normal derivatives on the rigid surfaces, and is the outgoing solution of equation (8) when the right side is replaced by $\delta(\mathbf{x} - \mathbf{y})\delta(t - \tau)$, and the integration is over all times τ and over the volume occupied by the vortex sources. In the acoustic far field ($|\mathbf{x}| \to \infty$) $B \to p/\rho_0$, and G may be replaced by its *compact* approximation, which is valid provided that the characteristic acoustic wavelength is large compared to the chord $2a$ of the blade, which is always the case when the Mach number is sufficiently small. For simplicity we make use of a Green function that neglects the influence of finite duct diameter on propagation, i.e., the dominant wavelength is assumed to be small compared to the duct diameter (or blade span). The inclusion of such effects (which, in addition, must take account of duct termination conditions) is not difficult in principle, but does not materially alter the fundamental nature of the blade–vortex interaction, and can be accomplished by minor modification of results given below. In Appendix A it is shown that the appropriate compact approximation is

$$G(\mathbf{x}, \mathbf{y}, t - \tau) \approx \frac{Y_1 \cos \Theta}{2\pi |\mathbf{x}| c_0}\, \delta'(t - \tau - |\mathbf{x}|/c_0), \qquad |\mathbf{x}| \to \infty, \tag{10}$$

where the prime denotes differentiation with respect to the argument of the delta function, $\cos \Theta = x_1/|\mathbf{x}|$ represents the dipole directivity of the radiated sound, Θ being the angle (shown in Figure 2(a)) between the observer direction (in $x_2 > 0$) and the blade normal, and

$$\begin{aligned} Y_1 &= \frac{\sqrt{(a^2 - y_3^2)}}{\ln[(4/b)\sqrt{(a^2 + \varepsilon^2 b^2 - y_3^2)}]} \mathrm{Re}(\ln[\xi/b + \sqrt{(\xi^2/b^2 - 1)}]), \qquad |y_3| < a, \\ &= 0, \qquad |y_3| > a, \end{aligned} \tag{11}$$

where $\xi = y_2 + \mathrm{i}y_1$.

In this formula, ε is a constant that exceeds $\frac{1}{4}$, but the precise value of which has little or no influence on the magnitude of the radiation (see Apendix A). The approximation is applicable to aeroacoustic sources located in the vicinity of the blade tip, indeed, the derivative with respect to $\mathbf{y}$ of $\mathrm{Re}\{\ln[\xi/b + \sqrt{(\xi^2/b^2 - 1)}]\}$ (which will be recognized as the two-dimensional approximation to the velocity potential of flow through the gap), is significantly different from zero only for $\mathbf{y}$ in the neighborhood of the gap. Y_1 vanishes for $|y_3| > a$, where the influence of the gap on sound generation is negligible.

3.2. THE RADIATED SOUND

There are two principal contributions to the aerodynamic sound integral (9). They correspond, respectively, to the direct radiation produced by the incident vortex alone, and to the sound generated by the vorticity shed from the blade tip.

For the incident vortex

$$\mathbf{\Omega} \wedge \mathbf{v} = \Gamma \mathbf{k} \wedge \mathbf{v}_\Gamma \delta(x_1 - x_0(t))\delta(x_2 - y_0(t)), \tag{12}$$

where $(x_0(t), y_0(t))$ is the position of the vortex at time t, calculated in section 2, and $v_\Gamma = (\mathrm{d}x_0/\mathrm{d}t, \mathrm{d}y_0/\mathrm{d}t, 0)$ is its translational velocity. Substituting into equation (9) we find

that the component p_Γ, say, of the far field acoustic pressure attributable to the vortex alone is given by

$$\frac{p_\Gamma}{\rho_0} = -\frac{\Gamma a^2 \beta \cos\Theta}{2\pi c_0 |\mathbf{x}|}\left[\frac{\mathrm{d}}{\mathrm{d}t}\,\mathrm{Re}\left(\frac{\mathrm{d}x_0/\mathrm{d}t - \mathrm{i}\,\mathrm{d}y_0/\mathrm{d}t}{\sqrt{(\xi_0^2 - b^2)}}\right)\right]_{[t]}, \qquad |\mathbf{x}|\to\infty, \tag{13}$$

where the quantity in square brackets is evaluated at the retarded time $[t] = t - |\mathbf{x}|/c_0$ (i.e., at the retarded position $\xi_0 = y_0 + \mathrm{i}x_0$ of the vortex), and β is a constant arising from the integration in equation (9) with respect to the chord-wise source co-ordinate y_3 over the interval $-a < y_3 < a$:

$$\beta = \int_{-1}^{1} \frac{\sqrt{(1-\lambda^2)}\,\mathrm{d}\lambda}{\ln[(4a/b)\sqrt{\{1 - \lambda^2 + \varepsilon^2(b/a)^2\}}]}. \tag{14}$$

The constant $\varepsilon \sim O(1)$, but its precise value is undetermined by the analysis presented in Appendix A. However, when $a \gg b$ the value of β is sensibly independent of ε to a good approximation. Thus, for $1 < \varepsilon < 5$, β is given correct to two significant figures as follows:

a/b	β
10	0·44
10^2	0·27
10^3	0·19

The vorticity (3) shed from the blade tip is distributed along the free streamline, and vorticity at distance s along the streamline from the tip translates at velocity $\mathbf{v} = V_c\mathbf{t}(s)$. where $\mathbf{t}(s) \equiv (t_1(s), t_2(s))$ is the unit tangent in the x_1–x_2 plane to the streamline. By making use of the Fourier integral representation (6) of $\gamma(t - s/V_c)$, the corresponding component p_γ of the acoustic pressure can be expressed in the form

$$\frac{p_\gamma}{\rho_0} \approx \frac{V_c a^2 \beta \cos\Theta}{2\pi c_0 |\mathbf{x}|}\int_{-\infty}^{\infty} -\mathrm{i}\omega\gamma_0(\omega)F(\omega)\,\mathrm{e}^{-\mathrm{i}\omega[t]}\,\mathrm{d}\omega, \qquad |\mathbf{x}|\to\infty, \tag{15}$$

where

$$F(\omega) = \int_0^\infty \mathrm{Re}\left(\frac{t_1(s) - \mathrm{i}t_2(s)}{\sqrt{(\xi_s^2 - b^2)}}\right)\mathrm{e}^{\mathrm{i}\omega s/V_c}\,\mathrm{d}s, \tag{16}$$

and $\xi_s = x_2(s) + \mathrm{i}x_1(s)$, where $(x_1(s), x_2(s))$ are the co-ordinates of a point distant s along the free streamline from the blade tip.

3.3. NUMERICAL RESULTS

Inspection of equations (13) and (15) indicates that the order of magnitude of the acoustic pressure is $\rho_0 v^2 M$, where v is a flow velocity and $M = v/c_0$. This is characteristic of an aeroacoustic dipole source. The dipole axis is normal to the blade, and its strength is equal to the unsteady lift exerted on the blade during the passage of the vortex [13].

The solid curve in Figure 5 represents a typical predicted acoustic pressure signature plotted as a function of the non-dimensional retarded time $V[t]/b$ for $b/a = 0{\cdot}1$, when the circulation of the incident vortex $\Gamma = \alpha V a$ and $\alpha = \pi/18$ (i.e., $\Gamma \approx 1{\cdot}75Vb$). This value of Γ corresponds approximately to the strength of a tip vortex shed by an airfoil of chord

$2a$ and angle of attack α ($\approx 10^\circ$). Time is measured from the instant at which the vortex passes through the gap, and the initial conditions have been chosen to ensure that $d/b = 0{\cdot}5$, where d is the distance of the vortex from the wall in the gap. The ordinate is $p(\mathbf{x}, t)/p_0$, where

$$p_0 = \frac{\rho_0 V^2 \Gamma a^2 \cos \Theta}{c_0 b^2 |\mathbf{x}|} \tag{17}$$

accounts for the characteristic dipole amplitude and directivity. The sound is generated predominantly when the vortex passes through the gap, during an interval of time of order b/V. Its wavelength is therefore of order $c_0 b/V \equiv a(b/a)/M$ ($M = V/c_0$), which is large relative to the blade chord provided that $M \ll b/a$.

Also plotted are the separate contributions p_Γ/p_0 (dotted curve) and p_γ/p_0 (dashed) of the sound generated by the incident vortex and the shed vorticity, respectively. For much of the time these pressures are approximately of opposite phase and tend to interfere destructively. In the analogous problem of thin airfoil theory, involving the interaction of a vortex with a trailing edge, when both the incident and shed vorticity are assumed to convect parallel to the airfoil at the *same* velocity, the cancellation is complete, and no sound is generated when the vortex passes by the trailing edge [15]. In the present case only partial cancellation occurs.

In Figure 6 is illustrated, for the same vortex strength Γ and for $b/a = 0{\cdot}1$, the dependence of the acoustic pressure on the ratio d/b. The numerical results of section 2 show that the maximum value of d/b for which the vortex penetrates the gap (and is not "reflected" as in the upper trajectory of Figure 3) is about 0·68, and as d/b approaches this value the amplitude of the acoustic radiation is seen to progressively increase. When d/b is small, however, the acoustic amplitude becomes very small, because the upwash induced on the blade by the vortex tends to be cancelled by that of an equal and opposite image vortex in the duct wall.

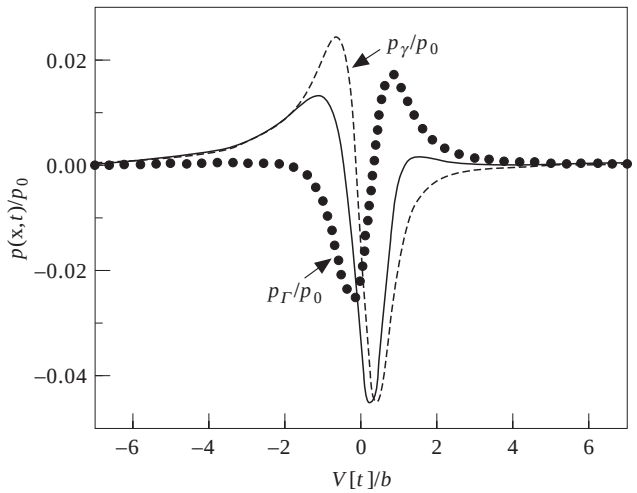

Figure 5. The acoustic pressure $p(\mathbf{x}, t)/p_0$ (——) plotted as a function of the non-dimensional retarded time $V[t]/b$ for $\Gamma = 1{\cdot}75Vb$, $b/a = 0{\cdot}1$ and $d/b = 0{\cdot}5$. ●●●●●, Direct radiation p_Γ/p_0 from the incident vortex; - - - -, radiation p_γ/p_0 from the shed vorticity.

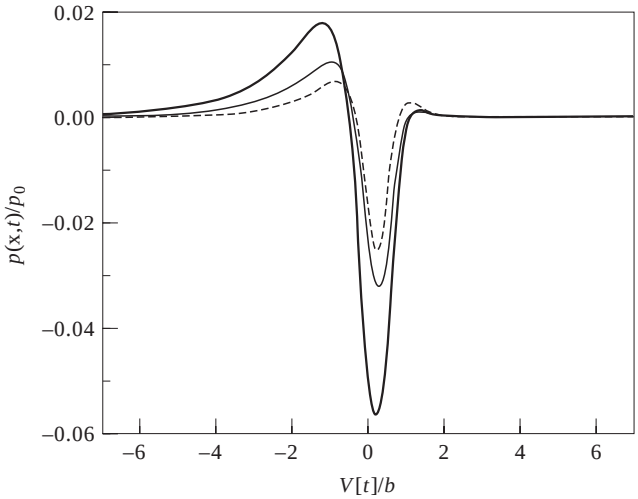

Figure 6. The dependence of the acoustic pressure $p(\mathbf{x}, t)/p_0$ on d/b when $\Gamma = 1{\cdot}75Vb$ and $b/a = 0{\cdot}1$. ——, $d/b = 0{\cdot}6$; ——, $d/b = 0{\cdot}4$; ---, $d/b = 0{\cdot}2$.

4. SIMPLIFIED ANALYTICAL APPROXIMATION

An entirely analytical treatment of the sound generation problem can be given in the approximation indicated schematically in Figure 7. Since the sound is produced primarily when the vortex is near the gap, its convection velocity is assumed to be constant and equal to V, the mean velocity in the gap, and the vortex path is taken to be rectilinear, at a fixed distance d from the duct wall. Similarly, the shed vorticity is assumed to convect at velocity V_c parallel to and distance b from the wall (above the free streamline of the wall jet in Figure 7).

When these assumptions are made most of the integrals in sections 2 and 3 can be evaluated analytically. Thus, the solution (7) of equation (4) for the circulation of the shed vorticity (where s now denotes distance from the blade tip in the x_1-direction), becomes

$$\gamma_0(\omega) = \frac{-(2\Gamma/\pi V)\sinh(|\omega|d/V)\mathrm{K}_1(|\omega|b/V)}{2\sinh(|\omega|b/V_c)\mathrm{K}_1(|\omega|b/V_c) + \pi\mathrm{i}\,\mathrm{sgn}(\omega)\mathrm{I}_1(|\omega|b/V_c)\exp(-|\omega|b/V_c)}, \qquad (18)$$

where K_1 and I_1 are modified Bessel functions [20], and $\gamma_0(-\omega) = \gamma_0^*(\omega)$, the asterisk denoting the complex conjugate.

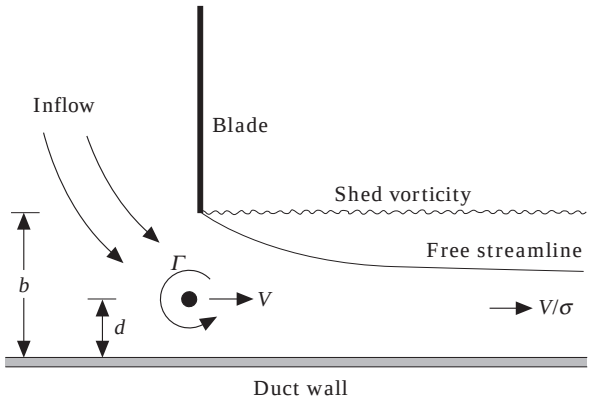

Figure 7. A simplified model of the blade–vortex interaction.

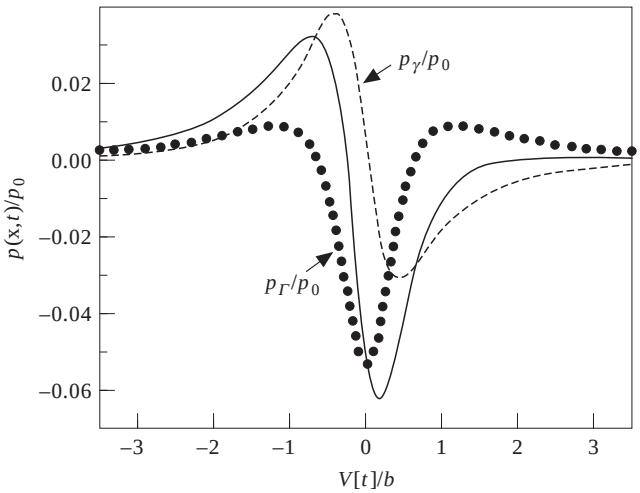

Figure 8. Predictions of the simplified approximation of section 4. The acoustic pressure $p(\mathbf{x}, t)/p_0$ (——) plotted as a function of the non-dimensional retarded time $V[t]/b$ for $\Gamma = 1{\cdot}75Vb$ and $d/b = 0{\cdot}5$. ●●●●●, Direct radiation p_Γ/p_0 from the incident vortex; - - - -, radiation p_γ/p_0 from the shed vorticity. $b/a = 0{\cdot}1$.

As $|\mathbf{x}| \to \infty$, the direct vortex sound p_Γ and the sound p_γ generated by the wake vorticity are found to be given by

$$\frac{p_\Gamma}{p_0}(\mathbf{x}, t) \approx \frac{-\beta b}{2\pi V}\mathrm{Re}\left[\frac{\partial}{\partial t}\left(\frac{b}{\sqrt{\{(d + \mathrm{i}V[t])^2 - b^2\}}}\right)\right], \tag{19}$$

$$\frac{p_\gamma}{p_0}(\mathbf{x}, t) \approx \frac{\beta}{2\pi^2}\left(\frac{V_c}{V}\right)^3 \int_{-\infty}^{\infty} \frac{\lambda[2\sinh(\lambda)\mathrm{K}_0(|\lambda|) - \mathrm{i}\pi \mathrm{I}_0(|\lambda|)\,\mathrm{e}^{-|\lambda|}]}{2\sinh(|\lambda|)\mathrm{K}_1(|\lambda|) + \pi\mathrm{i}\,\mathrm{sgn}(\lambda)\mathrm{I}_1(|\lambda|)\exp(-|\lambda|)}$$

$$\times \sinh\left(|\lambda|\frac{dV_c}{bV}\right)\mathrm{K}_1\left(|\lambda|\frac{V_c}{V}\right)\exp(-\mathrm{i}\lambda V_c[t]/b)\,\mathrm{d}\lambda, \tag{20}$$

where p_0 is defined in equation (17), and $[t] = t - |\mathbf{x}|/c_0$ is the retarded time. These are plotted as functions of $V[t]/b$ in Figure 8 for $b/a = 0{\cdot}1$ and $d/b = 0{\cdot}5$. The solid curve is the net acoustic pressure $(p_\Gamma + p_\gamma)/p_0$.

In this constant velocity approximation to the motion of the incident vortex the predicted direct acoustic pressure p_Γ is an even function of the retarded position $V[t]$ of the vortex. This symmetry is absent from the more general result of Figure 5 because of the accelerated motion of the vortex in the gap. However, there is good overall qualitative and quantitative agreement between the present approximation and the numerical results of Figures 5 and 6.

These results (and the more detailed predictions of section 3) indicate that the magnitude of the acoustic pressure is of characteristic order

$$\frac{10^{-2}\rho_0 V^2 \Gamma (a/b)^2}{c_0|\mathbf{x}|}.$$

The corresponding strength of the sound produced when the vortex is *severed* by the blade is [15]

$$\frac{\rho_0 U^2 \Gamma \sqrt{a/R}}{c_0|\mathbf{x}|},$$

where U is the relative velocity of the vortex and blade, and R is the radius of the vortex core. In practice, it is likely that V and U will be of the same order, and that, typically, $a/R \sim a/b \approx 5$–10. Thus, it appears that both mechanisms will produce sound of comparable orders of magnitude.

5. CONCLUSIONS

Discrete-vortex rotor blade interactions are important sources of sound and vibration in turbomachines. In this paper the methods of classical free streamline theory and the Lighthill acoustic analogy have been combined to investigate the canonical problem of the sound generated when a vortex is convected at low Mach numbers through the clearance between a square blade tip and a neighboring wall. The mean flow near the tip of the suction side of the blade has been modelled by a locally two-dimensional, potential flow wall jet, and vorticity shed from the tip in accordance with the unsteady Kutta condition has been assumed to convect at constant speed along the free streamline of the jet. The net unsteady force exerted on the blade during the interaction gives rise to a dipole sound source, in which the acoustic amplitude varies as $\rho_0 v^2 M$, where v is a typical velocity and $M = v/c_0$, and we have calculated the individual contributions to the radiation from the vortex and the blade-tip shed vorticity; the overall magnitude of the sound is comparable to that which would be produced if the vortex were to be "chopped" by the blade. The radiation is significant only when the distance of the vortex from the blade tip is less than about the clearance b between the tip and wall, and the wavelength of the generated sound is therefore of order b/M.

The numerical predictions are consistent with an alternative, simplified analytic model in which the convection velocity of the vortex relative to the blade is constant, and the shed vorticity translates at a fixed distance from the wall rather than along the free streamline of the wall jet.

ACKNOWLEDGMENTS

The research reported in this paper was sponsored by the Office of Naval Research under Grant N00014-93-1-0111 administered by Mr James A. Fein, and Grant N00014-95-1-0318 administered by Dr Patrick L. Purtell.

REFERENCES

1. N. A. Cumpsty 1977 *Transactions of the American Society of Mechanical Engineers*, *Journal Fluids Engineering* **99**, 278–293. A critical review of turbomachinery noise.
2. T. Y. Wu and G. T. Yates 1988 *David Taylor Research Center Contract Report N*61533-87-*M*-2981. Literature survey of flow noise generation and propagation in turbomachinery.
3. W. K. Blake 1986 *Mechanics of Flow-induced Sound and Vibration*, *Vol*. 2: *Complex Flow-Structure Interactions*. New York: Academic Press.
4. D. G. Crighton 1972 *Journal of Fluid Mechanics* **51**, 357–362. Radiation from vortex filament motion near a half plane.
5. F. Obermeier and T. von Schroeter 1988 *Journal of Acoustics* (France) **2**, 255–258. Aerodynamic sound generation by vortex motion through an aperture in an infinitely extended solid plate.
6. F. Obermeier and K.-Q. Zhu 1993 *Journal of Aircraft* **30**, 81–87. Sound generation by rotor–vortex interaction in low Mach number flow.
7. A. T. Hsu and J. C. Wu 1988 *American Institute of Aeronautics and Astronautics Journal* **26**, 621–623. Vortex flow model for the blade–vortex interaction problem.

8. D. R. Poling and L. Dadone 1987 *American Institute of Aeronautics and Astronautics Journal* **27**, 694–699. Blade–vortex interaction.
9. L. Roberts and D. J. Lee 1984 *Paper presented at a Workshop on Blade–Vortex Interactions*, *NASA Ames Research Center*, 29–31 *October*. An analysis of blade–vortex interaction noise.
10. S. Widnall 1971 *Journal of the Acoustical Society of America* **50**, 354–365. Helicopter noise due to blade–vortex interaction.
11. Y. Xue and A. S. Lyrintzis 1994 *American Institute of Aeronautics and Astronautics Journal* **32**, 1350–1359. Rotating Kirchhoff method for three-dimensional transonic blade–vortex interaction hover noise.
12. P. Cannell and J. E. Ffowcs Williams 1973 *Journal of Fluid Mechanics* **58**, 65–80. Radiation from line vortex filaments exhausting from a two-dimensional semi-infinite duct.
13. M. S. Howe 1991 *Proceedings of the Royal Society of London* **A433**, 573–598. On the estimation of sound produced by complex fluid structure interactions, with application to a vortex interaction with a shrouded rotor.
14. M. S. Howe 1975 *Journal of Fluid Mechanics* **71**, 625–673. Contributions to the theory of aerodynamic sound, with application to excess jet noise and the theory of the flute.
15. M. S. Howe 1988 *Proceedings of the Royal Society of London* **A420**, 157–182. Contributions to the theory of sound production by vortex-airfoil interaction, with application to vortices with finite axial velocity defect.
16. H. Lamb 1932 *Hydrodynamics*. Cambridge University Press; sixth edition, reprinted 1993.
17. L. M. Milne-Thompson 1968 *Theoretical Hydrodynamics*. London: Macmillan; fifth edition.
18. R. C. Dunne 1995 *M.S. Thesis*, *College of Engineering*, *Boston University*. Sound produced by a vortex interacting with a blade tip of a ducted rotor.
19. Y. C. Fung 1993 *An Introduction to the Theory of Aeroelasticity*. New York: Dover.
20. M. Abramowitz and I. A. Stegun 1970 *Handbook of Mathematical Functions*. U.S. Department of Commerce, National Bureau of Standards, Applied Mathematics Series No. 55; ninth corrected printing.

APPENDIX A: COMPACT GREEN FUNCTION

The compact Green function $G(\mathbf{x}, \mathbf{y}, t-\tau)$ for a stationary, rigid body with surface S is an approximate solution of equation (8) with outgoing wave behavior when the right side is replaced by the point source $\delta(\mathbf{x}-\mathbf{y})\delta(t-\tau)$ and when the normal derivatives $\partial G/\partial x_n$ and $\partial G/\partial y_n$ both vanish on S. If the mean flow Mach number is infinitesimal, so that convection of sound by the flow can be neglected,

$$G(\mathbf{x}, \mathbf{y}, t-\tau) = \frac{1}{4\pi|\mathbf{X}-\mathbf{Y}|}\,\delta(t-\tau-|\mathbf{X}-\mathbf{Y}|/c_0), \tag{A1}$$

where $X_i = x_i - \varphi_i^*(\mathbf{x})$, $Y_i = y_i - \varphi_i^*(\mathbf{y})$ and φ_i^* is the velocity potential of ideal incompressible flow that would be produced by rigid body motion of S at unit speed in the i-direction (so that X_i and Y_i are the potentials of flow past the fixed body having unit speed in the i-direction at large distances from S [14].

The compact Green function can be used to solve equation (8) in the presence of the rigid surface S provided that the characteristic acoustic wavelength of the sound is much larger than the diameter of the body (i.e., the blade chord in the problem of section 3) and either the observation point $\mathbf{x}$ *or* the source point $\mathbf{y}$ is many acoustic wavelengths from S. In that case the body behaves as a dipole source the characteristics of which are correctly determined by the compact approximation (A1). In the circumstances of this paper, where the blade tips are in motion at low Mach number, it was shown by Howe [13] that the sound produced by interaction with vorticity is the same as if the blades are taken to be at rest, provided the relative motion between the blade and vorticity is unchanged.

In the application of sections 3 and 4, the compact Green function is modified by the presence of the duct wall. We therfore consider first the determination of G when the wall

is absent, but the mirror image of the blade in the wall is inserted. In this case we have to determine $\mathbf{X}$ for an infinitely long, rigid strip of chord $2a$ containing a slit of width $2b$ in the interval $|x_2| < a$. Far from the slit we have [16, 17]

$$X_1 = \mathrm{Re}\,[-\mathrm{i}\sqrt{(z^2 - a^2)}], \quad X_2 = x_2, \quad X_3 = x_3 \qquad (z = x_3 + \mathrm{i}x_1). \tag{A2}$$

Very close to the slit, but at distances $\gg b$ from the leading and trailing edges ($x_3 = \pm a$) of the blade, X_1 must assume the form

$$X_1 \approx \frac{m(x_3)}{\pi}\,\mathrm{Re}\,(\ln\,[\xi/b + \sqrt{(\xi^2/b^2 - 1)}]), \qquad \xi = x_2 + \mathrm{i}x_1, \qquad |x_3 \pm a| \gg b. \tag{A3}$$

Here X_1 is the potential of a locally two dimensional flow through the slit, and $m(x_3)$ is the volume flux per unit length of the slit. Near the leading and trailing edges of the blade the flow represented by the exact form of X_1 will tend to be *around* the edges of the blade rather than through the slit, so that $m(x_3) \to 0$ as $x_3 \to \pm a$.

An approximate expression for the fundamental form of $m(x_3)$ can be obtained by straightforward matching of the limiting forms (A2) and (A3) within an intermediate range of distances from the slit. The details are given in reference [18], where it is shown that

$$m(x_3) \approx \frac{\pi\sqrt{(a^2 - x_3^2)}}{\ln\,[(4/b)\sqrt{(a^2 - x_3^2)}]}\,. \tag{A4}$$

This is singular near $|x_3 \pm a| = b(b/32a) \ll b$; i.e., very close to the leading and trailing edges of the blade where, however, the matching procedure becomes invalid. Since $m(x_3)$ must actually tend smoothly to zero at these edges, expression (A4) can be regularized by writing

$$\begin{aligned} m(x_3) &\approx \frac{\pi\sqrt{(a^2 - x_3^2)}}{\ln\,[(4/b)\sqrt{(a^2 + \varepsilon^2 b^2 - x_3^2)}]}, \qquad |x_3| < a, \\ &= 0 \qquad |x_3| > a, \end{aligned} \tag{A5}$$

where the regularization parameter $\varepsilon \sim O(1)$, but must exceed $\frac{1}{4}$ to remove the singularity.

Equations (A3) and (A5) determine the behaviour of the Green function for sources at points $\mathbf{y}$ very close to the slit. For the actual problem, involving the presence of the rigid wall at $x_2 = 0$, we use the method of images to find

$$G(\mathbf{x}, \mathbf{y}, t - \tau) \approx \frac{1}{4\pi|\mathbf{x}|}\left[\delta\left(t - \tau - \frac{|\mathbf{x}|}{c_0} + \frac{\mathbf{x}\cdot\mathbf{Y}}{c_0|\mathbf{x}|}\right) + \delta\left(t - \tau - \frac{|\mathbf{x}|}{c_0} + \frac{\mathbf{x}\cdot\bar{\mathbf{Y}}}{c_0|\mathbf{x}|}\right)\right], \qquad |\mathbf{x}| \to \infty,$$

where $\bar{Y}_1 = Y_1$, $\bar{Y}_2 = -y_2$ and $\bar{Y}_3 = y_3$. This is further simplified for compact source distributions in the vicinity of the gap by expanding the delta functions in powers of $\mathbf{Y}/c_o$ and $\bar{Y}/c_0$. The leading order terms in this expansion yield the dipole approximation

$$G(\mathbf{x}, \mathbf{y}, t - \tau) \approx \frac{1}{2\pi|\mathbf{x}|}\left(\frac{x_1 Y_1}{|\mathbf{x}|c_0} + \frac{x_3 y_3}{|\mathbf{x}|c_0}\right)\delta'(t - \tau - |\mathbf{x}|/c_0), \qquad |\mathbf{x}| \to \infty, \tag{A6}$$

where the prime denotes differentiation with respect to the argument.

The second term in the brace brackets of equation (A6) may be omitted for aeroacoustic source distributions that are independent of the chord-wise variable y_3, and this leads immediately to equation (10) of the main text.